Electron Attachment to the Gas-Phase DNA Bases Cytosine and Thymine

S. Denifl, S. Ptasińska, M. Probst, J. Hrušák,† P. Scheier, and T. D. Märk*

Institut fuer Ionenphysik, Leopold-Franzens Universität Innsbruck, Technikerstr. 25, A-6020 Innsbruck, Austria

Received: February 10, 2004; In Final Form: May 3, 2004

We present a detailed study on dissociative electron attachment (DEA) to isolated gas-phase cytosine (C) and thymine (T). The experimental setup used for these measurements is a crossed electron/neutral beam instrument combined with a quadrupole mass spectrometer. Electron attachment to these biomolecules leads to dissociation into various fragments without a hint of any measurable amount of stable C or T parent anions. The fragment anions with highest abundance are $(C-H)^-$ and $(T-H)^-$, respectively. Quantum chemical calculations were performed to calculate the electron affinities and binding energies of the different isomers of the (T−H) fragment. Besides $(C-H)^-$ and $(T-H)^-$, we observed five other fragment anions formed by DEA to cytosine and eight additional product anions were detected in the case of thymine. Ion efficiency curves were measured for all fragment anions in the electron energy range from about 0 to 14 eV. For mixtures of T or C with SF_6 or CCl_4 in the collision chamber, additional resonances close to 0 eV were observed, resulting from ion molecule reactions of SF_6^- or Cl^- with the respective biomolecule.

Introduction

The interaction of high-energy radiation (α-, *β*-, *γ*-rays or heavy ions) with human cell components creates secondary species (ions, radicals, electrons) in a large amount along the radiation track. For instance, 10^4 secondary electrons are produced per 1 MeV deposited energy.[1] These produced secondary electrons have typically initial kinetic energies up to 20 eV.[2] Within picoseconds, they are thermalized by successive inelastic collisions in the medium. Recently, Sanche and co-workers[3] showed that free-low-energy electrons induce single- and double-strand breaks in thin films of DNA. They observed a local maximum for the yield of DNA strand breaks at an incident electron energy of about 10 eV. They concluded that the dissociation of transient negative ion states of various components of DNA/RNA (bases, phosphate−sugar backbone, or surrounding water) initiates the DNA strand breaks and leads to this resonance of the DNA damage at 10 eV. According to the results of ref 3, it is worthy to study the properties of isolated DNA building blocks which are supposed to be the initial sites for strand breaks. In the present free electron attachment experiment, the interaction of low-energy electrons with isolated gas-phase DNA components has been studied thus avoiding environmental influence. Cytosine ($C_4H_5N_3O$) and thymine ($C_5H_6N_2O_2$) are bases of the gene sequence in DNA. The corresponding molecular structures are shown in Figure 1. In the DNA complex, thymine is paired with adenine via two hydrogen bonds, and cytosine is bound to guanine by three hydrogen bridges. Uracil (U) replaces T in RNA and has already been the subject of several studies recently.[4−7]

Dissociative electron attachment (DEA) to a molecule M like cytosine and thymine starts initially with the formation of $(M^-)^*$, a transient negative ion (TNI). Depending on the autodetachment lifetime, the TNI can decay into a fragment anion and corresponding neutral fragments. The ensuing fragment anions often carry the signature of the TNI, that is, in the position of the resonances. The formation of TNI states of cytosine (C) and thymine (T) was already studied by Burrow and co-workers using electron transmission spectroscopy.[7] They concluded that an anion state is formed most likely by occupation of the lowest empty π^* molecule orbital of C and T. In ref 7, only the electron occupation of valence orbitals was investigated and not anions states, where the electron is weakly trapped in the dipole field of the DNA base. Dipole bound parent anions of DNA bases have been investigated in Rydberg electron transfer[8−11] or negative photoelectron spectroscopy[12−14] studies. The group of Schermann and co-workers[8] observed stable dipole bound parent anions of adenine, thymine, and Uracil formed by Rydberg electron transfer. The formation of dipole bound anions is a result of the high dipole moment of these molecules which is larger than 2.5 D.[15] Stable valence bound anions were only detected for $(M-H)^-$. However, Rydberg electron transfer to a mixed Uracil/argon cluster[9] enables the formation of valence bound parent anions of Uracil after evaporation of the argon atoms from the cluster. Bowen and co-workers[13] investigated the transition from dipole bound to covalent ion by studying different solvents with Uracil. In the Uracil/xenon complex, it is possible to observe dipole and covalent bound anions simultaneously in the photoelectron spectrum. Schiedt and co-workers[14] performed anion spectroscopy of Uracil, thymine, and cytosine. They determined the valence adiabatic electron affinity of differently sized mixed X/water clusters (X= U, T, C) and

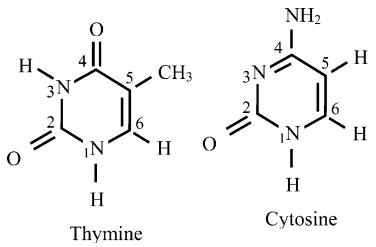

Figure 1. Molecular structure of cytosine and thymine.

* Corresponding author. E-mail: Tilmann.Maerk@uibk.ac.at. Also adjunct professor at Department of Plasma Physics, Comenius University, SK-84248 Bratislava, Slovakia.

† Permanent address: J. Heyrovsky Institute of physical chemistry AV CR, Dolejškova 3, 182 23 Prague, Czech Republic.

10.1021/jp049394x CCC: $27.50
Published on Web 07/14/2004

extrapolated to the monomer value. The photoelectron−photodetachment spectrum of $C/(H_2O)_2$ cluster showed also dipole bound states of two possible tautomers of cytosine (amino-oxo and amino-hydroxy cytosine). Adamowicz and co-workers[16] studied theoretically the stability of covalent and dipole bound anions of cytosine taking into account these two possible tautomers of cytosine.

A variety of theoretical calculations of both adiabatic (AEA) and vertical electron affinities (VEA) of C and T has been published[17−22] (please note also a recent study on the EAs of adenine−thymine and guanine−cytosine base pairs[23]). The AEA of earlier theoretical calculations around 1 eV[24] agreed well with experimental determinations of the AEA on the basis of the reduction potential[25] but seem to be questionable.[19] All reliable calculations lead to similar values for the electron affinities taking into account an uncertainty of typically about ±0.1 eV. The VEA of C and T are negative (typical values are −0.5 eV and −0.3 eV, respectively[21]) while the AEA are very close to zero eV and with slightly positive or negative values depending on the method of calculation (mostly determined by the size of the basis sets used). These differences between adiabatic and vertical electron affinity reflect the substantial relaxation of the molecules during the electron attachment event.

Chen and Chen[26] constructed Morse potential curves for both molecules on the basis of experimental data. They also report negative ion mass spectra determined with negative chemical ionization mass spectrometry where exclusively dehydrogenated DNA and RNA bases were obtained.

Free electron attachment experiments to gas-phase cytosine and thymine were first performed by Huels et al.[27] using a trochoidal electron monochromator. They observed stable parent anions of T and C. In addition, they reported the formation of seven smaller fragment anions (<43 Da) via DEA to T. For the cytosine molecule, they also observed larger fragment ions such as $(C-2H)^-$ and $(C-NH_2)^-$. Recently, Gohlke and Illenberger[28] questioned the existence of stable parent anions published by the same group before in ref 27. Abouaf et al.[29] investigated dissociative electron attachment to thymine and 5-bromouracil using a hemispherical monochromator in combination with a time-of-flight mass spectrometer. In their article, they report the formation of $(T-H)^-$. They proposed that the narrow peak structure of $(T-H)^-$ observed in their experiment arises from the vibrational structure of predissociated (dipole) anion states by Π* valence resonant states (see also a recent work which suggests a similar mechanism in Uracil[30]).

Another recent electron attachment experiment with C and T studied the anion formation in the condensed phase,[31] that is, anion desorption from thin films of C and T in the electron energy range from about 5−40 eV. In contrast to gas-phase experiments, only low mass fragment anions have been observed. They are formed via DEA resonantly below 15 eV and for higher electron energies in nonresonant processes such as dipolar dissociation, respectively. The resonance structure of the desorption yields are similar with that of the DNA strand break yields observed by Sanche and coworkers[3] which indicates that initial DEA of DNA components is a possible source for strand breaks of DNA.

Like in the previous investigations,[27−29] the present experiment is a standard crossed neutral/electron beam setup, however, having a better energy resolution and higher sensitivity. We already published first results concerning the most abundant anions $(C-H)^-$ and $(T-H)^-$ in a recent letter[32] and in contrast to ref 27 we did not detect any parent anions. In the present report, we discuss our measurements in more detail and present

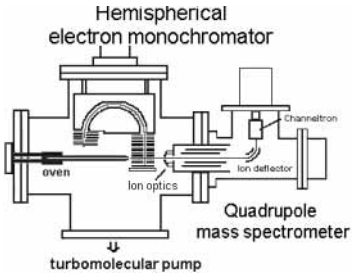

Figure 2. Schematic view of the experimental setup.

all fragment anions formed via DEA to cytosine and thymine measured within our detection limit. We also present quantum chemical calculations based on the MP2 and B3LYP levels of theory and the G2MP2 method. The binding energy (BE(T−H,H)) for each hydrogen atom of the thymine molecule, the electron affinity (EA) of T, and the EA of all possible (T−H) radicals have been determined. From these data, the energy threshold E_n for different isomers of $(T-H_n)^-$ is calculated by

$$E_n = \mathrm{BE}(T-H_n,H_n) - \mathrm{EA}(T-H_n)\ (n = 1, 3, H/CH_3, 6) \quad (1)$$

with n the position of the hydrogen in the thymine molecule (see Figure 1).

Experimental Section

For the present DEA experiments, a crossed electron/neutral beam apparatus is used (for more details see ref 33 and Figure 2). The neutral beam is produced by heating a resistively heated oven containing C or T powder to a temperature of 180−200 °C, respectively. The powders have a purity of 99.5% and were purchased from Sigma Aldrich. The evaporated molecules effuse through a capillary (1 mm diameter) into the collision chamber where they interact with the monochromatized electron beam. The electrons are produced by a filament and are accelerated with a lens system into a hemispherical electrostatic field analyzer, where the electron energy resolution is set to a value of 90−120 meV. In the past, we achieved with this electron monochromator a best value of 35 meV for the electron energy resolution. The presently used settings are a compromise between signal intensity and electron energy resolution. After the hemispheres, the electrons are accelerated with a second lens system to the desired energy and focused into the collision chamber. The formed anions are extracted into the quadrupole direction by a weak electric field and mass analyzed with a high-resolution quadrupole mass spectrometer. The ion current is amplified by a channeltron type secondary electron multiplier operated in a pulse counting mode and recorded by a computer. The main chamber has a residual gas pressure of 7×10^{-6} Pa and is heated to a temperature of 100 °C to (i) prevent condensation of the biomolecules on cold surfaces and to (ii) maintain stable conditions of the experimental setup for sufficiently long times.

With this setup, the ion current for mass-selected anions is recorded as a function of the electron energy. The energy scale is determined by measuring the ion yield of a calibration gas under identical conditions. The following two attachment reactions are typically used for calibration:

$$SF_6 + e \rightarrow SF_6^- \quad (2)$$

$$CCl_4 + e \rightarrow Cl^- + CCl_3 \quad (3)$$

The ion yields of the anions formed via reactions 2 and 3 exhibit

a sharp peak at 0 eV formed via s-wave attachment to the corresponding neutral molecules.[34,35] The electron energy resolution is determined as the full-width at half-maximum of the zero eV peak. Reaction 3 leads to a second peak (Gaussian shape) in the ion yield at an electron energy of 0.8 eV. We use the well-known cross-sectional value of this resonance[36−38] to obtain measures for the absolute cross section from our relative ion efficiency measurements. We measure reaction 3 and the biomolecules under identical conditions. For this purpose, we introduce the calibration gas into the oven where the biomolecules are vaporized. Thereby both molecules will be introduced simultaneously into the collision chamber and the same electron beam (electron energy, electron current) interacts with the calibrant and biomolecule. We try to achieve the same partial gas density of CCl_4 and C or T; however, the real value of the partial pressure of the biomolecule may be 1 order of magnitude higher since these molecules adsorb easily on surfaces.[39] For more details about the inherent deficiencies of this method including ion discrimination due to kinetic energy release, see ref 40.

Results

(a) Cytosine. In the present experiments, the formation of six fragment ions formed via DEA to cytosine was observed:

$$e + C \leftrightarrow (C)^{-*} \rightarrow (C-H)^- + H^{\bullet} \quad (4a)$$

$$\rightarrow (C_3H_3N_2)^- + \text{fragments} \quad (4b)$$

$$\rightarrow (C_3HN_2)^- + \text{fragments} \quad (4c)$$

$$\rightarrow (OCN)^- + \text{fragments} \quad (4d)$$

$$\rightarrow (CN)^- + \text{fragments} \quad (4e)$$

$$\rightarrow O^-/NH_2^- + \text{fragments} \quad (4f)$$

Electron attachment to cytosine has been studied in the electron energy range from about zero to 14 eV. Figure 3 and Figure 4 show the ion yields of all fragment anions and the positions of all resonances observed are listed in Table 1. In our measurements, we were not able to observe any traces of parent anions because the lifetime of the TNI is apparently too short with respect to autodetachment and dissociation. The ion yield obtained at the mass of the parent can be fully ascribed to the expected isotopomer of $(C-H)^-$. Dehydrogenated cytosine is the most abundant fragment anion (see Figure 3a) with a maximum cross section of 2.3×10^{-20} m^2 which is very close to the cross-sectional value of $(U-H)^-$.[5,6,32] The resonance with the highest intensity is formed at an electron energy of 1.51 eV. Other resonances visible in the $(C-H)^-$ ion yield are located at 0.03, 1.1, and 5.19 eV.

The binding energies BE (cytosine-H,H) of all N−H sites and the EA for the corresponding different (C−H) isomers were calculated by Rodgers et al.[41] The AM1 and PM3 semiempirical methods were used in this work and it was found that AM1 generally produces more accurate values. The calculated minimum energy threshold for $(C-H)^-$ with removal of hydrogen from the ^{1}N−H site is 1.09 eV (AM1) and 0.63 eV (PM3) whereas the threshold for formation of $(C-H)^-$ by removal of the hydrogen from the NH_2 group is at least 0.3 eV higher. The present onset for the $(C-H)^-$ ion yield is at 0.94 eV whereas the small contribution close to 0 eV can be ascribed to a hot band transition, that is, the anion formation starts from a vibrationally excited molecule.[42] Chen et al.[43] used AM1-MCCI semiempirical calculations which should be somewhat more accurate than those employed in ref 41 and they observed a minimum threshold of 0.7 eV for removal of the hydrogen from the N−H site. To our knowledge, there are no high-level ab initio calculations so far available on the bond dissociation energies of C.

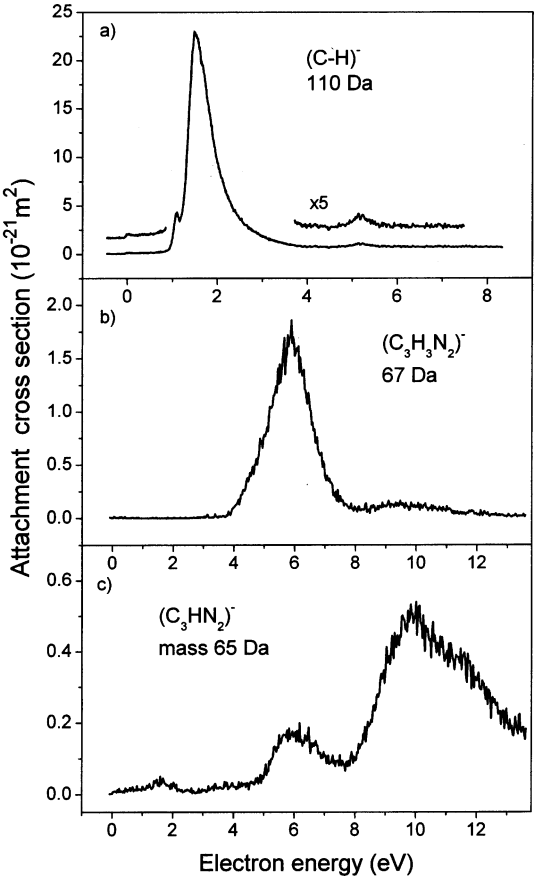

Figure 3. Ion yield of $(C-H)^-$, $(C_3H_3N_2)^-$, and $(C_3HN_2)^-$ formed via DEA to cytosine. The absolute cross-sectional scale was estimated from the known cross section of Cl^-/CCl_4 measured under the same conditions with an accuracy of 1 order of magnitude.

Electron transmission spectroscopy[7] reveals a temporary negative ion state of cytosine at an electron energy of 1.53 eV where an electron occupies an empty π^* orbital. The main peak of the $(C-H)^-$ ion yield in the present study is located close to this electron energy (i.e., at 1.51 eV). Huels et al.[27] reported in their electron attachment experiments to C an intact parent anion. They reported a shape for the ion yield as a function of the electron energy which is very similar to the present $(C-H)^-$ yield. A more recent study[44] performed with the same apparatus shows $(C-H)^-$ formation in agreement with the present results.

The anion formed via DEA to C with the second highest abundance is $(C_3H_3N_2)^-$ at mass 67 Da. The ion yield shows two resonances at 5.88 eV and 9.5 eV. The estimated cross section of the first peak has a value of 1.7×10^{-21} m^2. Two mass units below the $(C_3H_3N_2)^-$ we were able to detect $(C_3HN_2)^-$ which has a maximum cross section of 5.5×10^{-22} m^2 at its most abundant resonance at 10.03 eV. This fragment anion is also formed at other electron energies exhibiting peaks at 1.61 and 6.06 eV. At similar electron energies, resonances of $(OCN)^-$ are observed (2.12, 5.98, and 9.87 eV) although this ion is formed with a two times higher cross section of 1.3×10^{-21} m^2. The ion yield of O^-/C shows no significant formation of this fragment anion below the electron energy of 4 eV. The maximum of the first resonance is located at 5.74 eV.

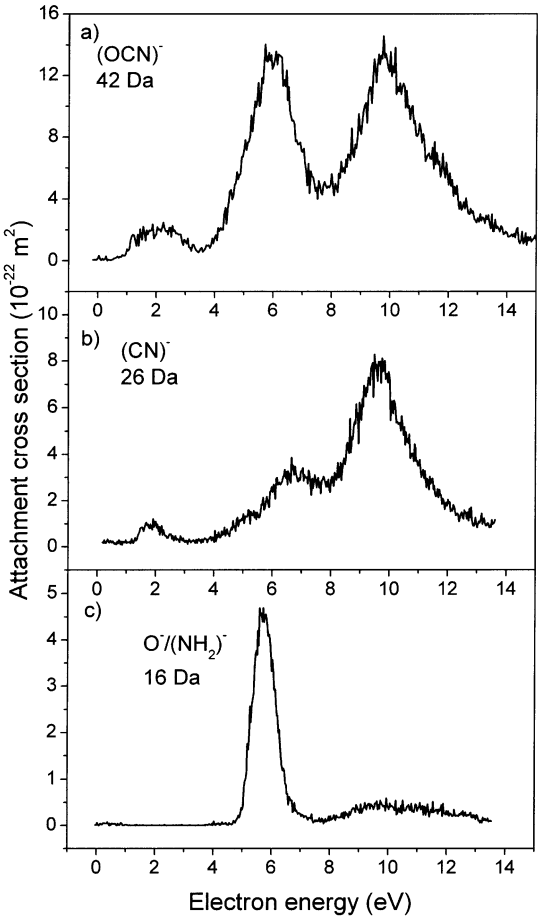

Figure 4. Ion yield of $(OCN)^-$, $(CN)^-$, and $O^-/(NH_2)^-$ formed via DEA to cytosine. The absolute cross-sectional scale was estimated from the known cross section of Cl^-/CCl_4 measured under the same conditions with an accuracy of 1 order of magnitude.

TABLE 1: Electron Energy Position (in eV) of Resonances for the Fragment Ions Formed via DEA to Cytosine[a] ($C_4H_5N_3O$)−111 Da

$(C-H)^-$ 110 Da	$(C_3H_3N_2)^-$ 67 Da	$(C_3HN_2)^-$ 65 Da	$(OCN)^-$ 42 Da	$(CN)^-$ 26 Da	$O^-/(NH_2)^-$ 16 Da
0.03 (0.1)	5.88 (4.5)	1.61	2.12 (1.0)	1.86 (1.2)	5.74 (2.3)
1.1 (1.4)	9.5 (7.3)	6.06	5.98 (5.0)	6.77 (5.1)	9.64 (3.8)
1.51 (5.3)		10.03	9.87 (7.7)	9.61 (7.8)	10.89 (5.2)
5.19 (6.9)					(7.4)
					(9.2)

[a] The present values are compared with values reported in ref 27 (in brackets), where available. Furthermore, the position of resonances for C^- observed by ref 27 are compared with those of $(C-H)^-$ (see text). Additional anions, observed in ref 27, but are absent in the present measurement, are not included.

The shape (position and relative heights of resonances) of the anion efficiency curves of all fragment anions of lower masses differ, in some cases substantially, from the spectra reported by Huels et al.[27] (see Table 1).

A comparison of the present ion yields and the positions of resonances suggest common precursor states for certain fragment ions. The fragment ions $(C_3H_3N_2)^-$, $(C_3HN_2)^-$, $(OCN)^-$, and O^- exhibit resonances around 6 and 10 eV, thus indicating the initial formation of two temporary negative ion states that subsequently dissociate with certain probabilities into these fragment anions. Within our detection limit, we were not able to observe other fragments of DEA to cytosine, like $(C-2H)^-$ or $(C-NH_2)^-$ that were mentioned in ref 27.

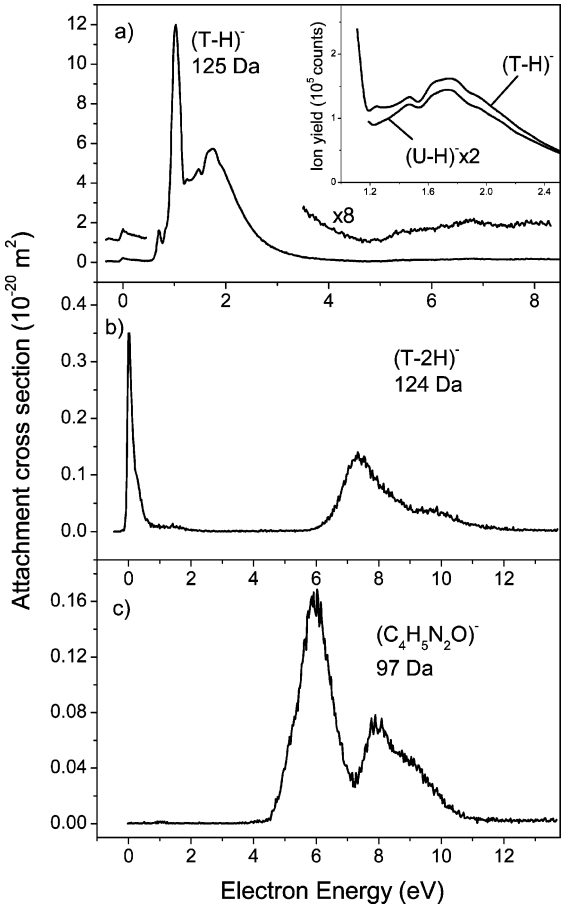

Figure 5. Ion yield of $(T-H)^-$, $(T-2H)^-$, and $(C_4H_5N_2O)^-$ formed via DEA to thymine. The absolute cross-sectional scale was estimated from the known cross section of Cl^-/CCl_4 measured under the same conditions with an accuracy of 1 order of magnitude. The insert in Figure 5a shows the peak structure of $(T-H)^-$ and $(U-H)^-$ measured with high resolution and accuracy in the electron energy range from about 1.1 eV to 2.4 eV. The $(T-H)^-$ ion yield reveals an additional peak at 1.24 eV.

(b) Thymine. Free-electron attachment to T leads to the following reaction channels observed within our detection limit:

$$e + T \leftrightarrow (T)^{-*} \rightarrow (T-H)^- + H^\bullet \quad (5a)$$

$$\rightarrow (T-2H)^- + 2H \quad (5b)$$

$$\rightarrow (C_4H_5N_2O)^- + \text{fragments} \quad (5c)$$

$$\rightarrow (C_2H_3N_2O)^- + \text{fragments} \quad (5d)$$

$$\rightarrow (C_3H_2NO)^- + \text{fragments} \quad (5e)$$

$$\rightarrow (C_3H_4N)^- + \text{fragments} \quad (5f)$$

$$\rightarrow (OCN)^- + \text{fragments} \quad (5g)$$

$$\rightarrow (CN)^- + \text{fragments} \quad (5h)$$

$$\rightarrow (O)^- + \text{fragments} \quad (5i)$$

Because of higher vapor pressure of T, the intensity of the neutral beam was higher than in C; thus, the signal-to-noise ratio is better for this molecule. Like in C and Uracil, no measurable amount of a parent anion was observed. The ion yield of $(T-H)^-$ is shown in Figure 5a. The peak structure exhibits six peaks (see Table 2a for exact peak positions) and

TABLE 2: Electron Energy Position (in eV) of Resonances for the Fragment Ions Formed via DEA to Thymine ($C_5H_6N_2O_2$)−126 Da

(a) Fragment Ion Mass > 67 Da[a]

$(T-H)^-$ 125 Da	$(T-2H)^-$ 124 Da	$(C_4H_5N_2O)^-$ 97 Da	$(C_2H_3N_2O)^-$ 71 Da	$(C_3H_2NO)^-$ 68 Da
0.04 (0.18)	0	5.95	8.53	6.71
0.7 (3.4)	1.41	7.96		8.58
1.02 (5.2)	7.39			
1.24	9.49			
1.47				
1.74				
5.4				
6.8				
7.8				

(b) Fragment Ion Mass < 67 Da[b]

$(C_3H_4N)^-$ 54 Da	$(OCN)^-$ 42 Da	$(CN)^-$ 26 Da	O^- 16 Da
7.06	2.33 (0.2)	6.94 (0.28)	9.8 (1.8)
	6.81(2.8)	8.41 (4.8)	12.36 (3.2)
	7.91 (4.6)	(6.4)	(4.5)
	9.5 (5.8)	(7.8)	(6.6)
	(7.7)	(8.7)	

[a] The present values for $(T-H)^-$ are compared with values for T− reported in ref 27 (see text). [b] The present values are compared with values reported in ref 27, where available. Additional anions observed in ref 27 in this mass range, but absent in the present measurement, are not included.

additional shoulders at 0.84 and 1.65 eV. ETS experiments[7] revealed a transient negative ion state of T at an electron energy of 1.71 eV which was ascribed to a π^* resonance. At this energy, we observe a broad peak in the attachment curve of $(T-H)^-$. The shape of the ion yield is very similar to the $(U-H)^-$ yield;[5,6,32] however, the presently estimated cross section for $(T-H)^-$ of 1.2×10^{-19} m^2 is approximately 4 times higher than for $(U-H)^-$. We measured the ion yield of $(T-H)^-$ and $(U-H)^-$ from the electron energy of about 1 eV to 2 eV for a very long time to reduce statistical noise below 0.3% (i.e., at each data point at least 10^5 ions were collected). The only difference in the relative cross-sectional curves is an additional small feature at 1.24 eV in the ion yield of $(T-H)^-$ (see insert in Figure 5a). Like for $(C-H)^-$, the additional small contribution near 0 eV in the $(T-H)^-$ ion yield can be ascribed to a hot band transition. However, a part of this signal close to 0 eV is also resulting from the loss of two hydrogen atoms (from the energetic point of view it has to be a H_2 molecule) from a T molecule that contains one ^{13}C isotope.

Abouaf et al.[29] observed in their electron attachment experiments with thymine a quite similar ion yield for $(T-H)^-$ although the ion yield is more pronounced near 0 eV than in the present study. This difference can be explained by an artifact peak which also appears when the oven used for the evaporation of thymine was completely empty.[45] Abouaf et al. also gave a rough estimation of the $(T-H)^-$ absolute cross section in ref 29. They give a lower limit of 10^{-19} m^2, which agrees quite well with the presently determined value. The positions of the resonances given in ref 29 are approximately 100 meV lower than in the present measurements. Like in cytosine, Huels et al.[27] observed in their measurements a long-lived parent anion of thymine. Like already discussed in a previous letter about DEA to C and T,[32] the $(T)^-$ ion yield (at 126 Da) presented by ref 27 could rather be due to SF_5^-/SF_6 (127 Da)[35,46] since SF_6 was used for calibration of the energy scale and introduced throughout the experiment. In addition, the cross section determined by Huels et al. for the parent anion of thymine was in the range of 10^{-18} m^2. This is about 1 order of magnitude larger than the $(T-H)^-$ cross section determined in the present investigation, however, very close to the cross section of SF_6^-/SF_6 mentioned in ref 46.

TABLE 3: Bond Dissociation Energies BE Required for the Removal of an H Atom from Neutral Thymine, Adiabatic Electron Affinities (AEA) of the Resulting Neutral (T−H) Isomers and Resulting Threshold Energies BE-EA as Calculated by Various Quantum Chemical Methods[a]

	B3LYP/ 6-311++G**			MP2/ 6-311+G(3df,2p)			G2MP2		
	BE	EA	BE−E A	BE	EA	BE−EA	BE	EA	BE−EA
^{1}N−H	4.9	3.2	1.7	5.0	3.9	1.1	4.4	3.5	0.9
^{3}N−H	5.1	3.7	1.4	5.9	4.3	1.6	5.8	4.5	1.3
CH_2−H							4.5	2.9	1.6
^{6}C−H	4.8	2.6	2.2	5.3	2.7	2.6	4.9	2.7	2.2

[a] The energies are given in eV and the accuracy is estimated to be about ±0.1 eV.

For thymine, we performed B3LYP[22] and MP2[47] calculations with large basis sets (using the basis sets 6-311++G** and 6-311+G(3df,2p), respectively[48,49]) as well as calculations with the G2MP2[50] method and determined bond dissociation energies of all different hydrogen atoms as well as the electron affinities EA of the corresponding (T−H) isomers. The results are listed in Table 3. The agreement between the different methods of calculation is reasonably good. Energetically most favorable is the removal of the hydrogen from the 1N site. The threshold energy agrees also with the presently observed onset of the $(T-H)^-$ ion yield within the uncertainty of the calculation of about ±0.1 eV. Furthermore, DEA experiments to partially deuterated T reveal that the $(T-H)^-$ anion is exclusively formed by removal of hydrogen from the nitrogen sites.[44,51] For the electron affinity of T, we obtained 0.15 eV (B3LYP), −0.39 eV (MP2), and −0.14 eV (G2MP2), respectively. All our calculations were performed using the G98 set of programs.[52]

Like for cytosine, previous determinations of the binding energy BE(T−H,H) and EA for different (T−H) isomers were performed by Rodgers et al.[41] and Chen et al.[43] using semiempirical methods. The latter ones obtained the minimum threshold energy of 0.5 eV for the ^{1}N site and 1.3 eV for the ^{3}N site. The values calculated by ref 41 were similar when the AM1 method was used (^{1}N: 0.6 eV, ^{3}N: 1.3 eV, respectively), whereas the PM3 method tends to result in a lowering of the thresholds of about 0.3 eV. The present calculations are more reliable than the previous determinations using semiempirical methods[41,43] because of the higher accuracy of ab initio calculations[53,54] used here.

In addition to $(T-H)^-$, we measured the ion yields of eight additional fragment anions formed via DEA to thymine. The corresponding ion yields are shown in Figures 5−7. In Table 2, the values for the center of the resonances are listed. $(T-2H)^-$ (Figure 5b) exhibits three peaks including a well-pronounced 0 eV resonance. This is in contrast to Uracil[6] where the $(U-2H)^-$ yield close to 0 eV is much weaker and presumably an artifact peak. DEA experiments with partially deuterated T show site selective dissociation for $(T-2H)^-$ formation,[51] that is, the formation of the various resonances can be ascribed to the removal of hydrogen from certain sites. The ion yield at mass 97 Da which is identified as the fragment ion $(C_4H_5N_2O)^-$ exhibits two peaks and a shoulder at an energy of 8.91 eV. The fragment anions $(C_2H_3N_2O)^-$ at mass 71 Da and $(C_3H_2NO)^-$ at mass 68 Da have the most intense resonance at an electron energy of about 8.5 eV which indicates a common TNI precursor state for both anions. Another common resonance

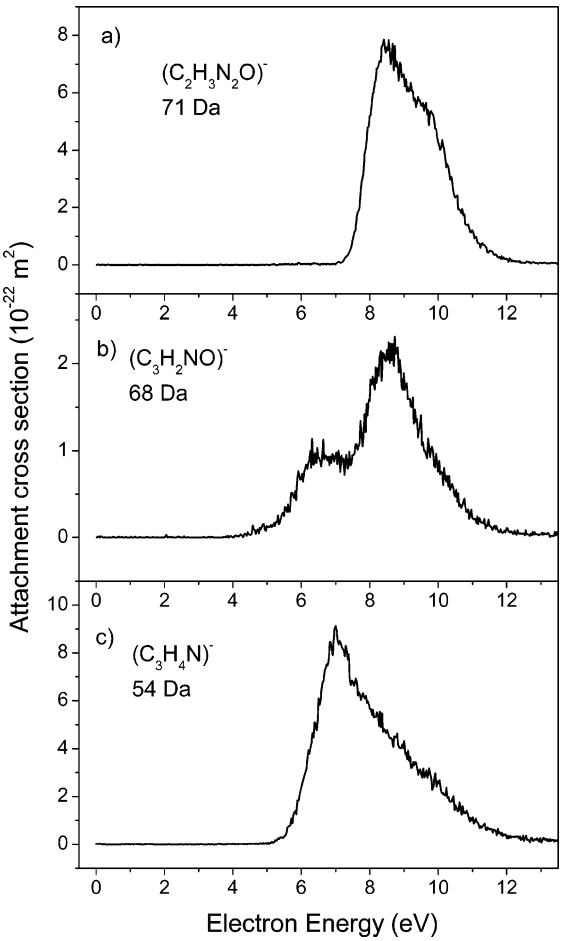

Figure 6. Ion yield of $(C_2H_3N_2O)^-$, $(C_3H_2NO)^-$, and $(C_3H_4N)^-$ formed via DEA to thymine. The absolute cross-sectional scale was estimated from the known cross section of Cl^-/CCl_4 measured under the same conditions with an accuracy of 1 order of magnitude.

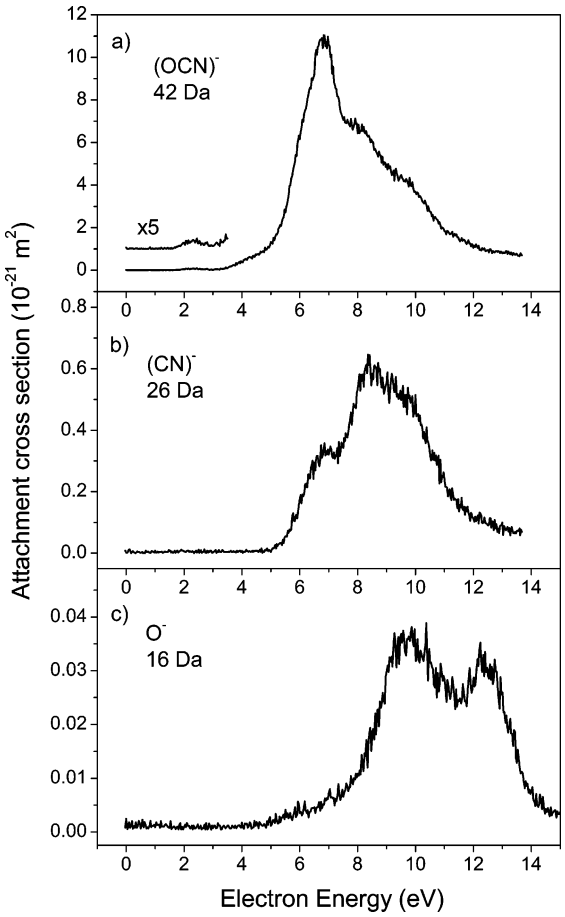

Figure 7. Ion yield of $(OCN)^-$, $(CN)^-$, and O^- formed via DEA to thymine. The absolute cross-sectional scale was estimated from the known cross section of Cl^-/CCl_4 measured under the same conditions with an accuracy of 1 order of magnitude.

was observed at 7 eV for the fragment anions at mass 54 Da, $(C_3H_4N)^-$, and 42 Da, $(OCN)^-$. The latter one has at the electron energy of about 2.3 eV a first very weak resonance and is formed more efficiently at electron energies larger than 5 eV exhibiting three additional resonances. At the apparent mass of $(ONCH)^-$, we observe anion signal that has the same shape as $(OCN)^-$, however, with a much lower intensity which perfectly matches with the isotope abundance of $(O^{13}CN)^-$ (agreement better than 2%). The ion yield of CN^- reveals a very similar peak structure as $(C_3H_2NO)^-$ except for a slight shift to higher energies and the appearance of a shoulder at the high-energy side of the maximum resonance. Furthermore, the partial cross section for CN^- is 3 times higher than for $(C_3H_2NO)^-$. The anion O^- is effectively formed only at energies above 8 eV with the corresponding peak maxima at 9.8 and 12.36 eV. The formation of H^-/T was briefly mentioned in ref 27 and we measured for the occurrence of this fragment anion three resonances at 5.4, 6.8, and 8.2 eV. A more detailed analysis of this fragment anion channel will be given elsewhere.[55]

Like in C, the position and relative height of the resonances of fragment anions smaller than $(T-H)^-$ differ in some cases substantially from the value published by Huels et al. (see Table 2).

The present ion yields observed for the variety of fragments from C and T differ substantially from each other. However, this result can be explained by the different molecular structure of both molecules, that is, different constituents outside the ring and the additional π-bond between ^{3}N and ^{4}C in cytosine. The ion efficiency curves of corresponding fragment ions formed via DEA to T and Uracil[6] reveal more common features. For instance, the $(T-H)^-$ and $(U-H)^-$ ion signals have exactly the same shape except a narrow small additional peak at around 1.24 eV for thymine. The relative attachment cross section of the $(C_3H_2NO)^-$ fragment is also practically the same for both molecules. Other fragment anions from U and T have only the main resonance in common like $(OCN)^-$ and O^-. The only difference in the molecular structure of T and U is a methyl group attached to the ^{5}C position in T whereas U has a hydrogen connected to this carbon atom. Thus, it is surprising that, although the ring structure is the same for T and U, DEA including ring dissociation leads to the formation of anions which are exclusively formed for T or U, for example, $(C_2H_3N_2O)^-$/T, $(C_3H_4N)^-$/T, $(C_3HNO)^-$/U, and $(C_2H_3N)^-$/U, respectively.

(c) Ion Molecule Reactions of Cytosine and Thymine. As in Uracil,[5,6,32] we observed that cytosine and thymine are able to react with anions of calibrant gases such as CCl_4 or SF_6 (see also a recent report about dissociative electron-transfer reactions of SF_6^- with adenine[56]). The present setup enables such interactions because the calibration gas and the biomolecules are introduced simultaneously through a capillary into the collision chamber. We have already described briefly the effect of such anion molecule reactions to the ion yield of $(C-H)^-$ and $(T-H)^-$ in our previous letter about EA to T and C.[32] In the presence of CCl_4 or SF_6 molecules and C or T in the collision chamber, we observe the following anion−molecule

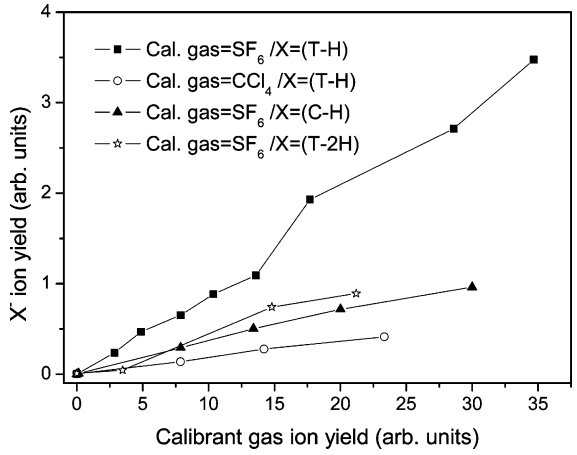

Figure 8. Dependence of the X^- ion yield (X = (T−H), (C−H), and (T−2H)) on the calibration gas anion signal at an electron energy of about 0 eV. As calibration gas, either SF_6 or CCl_4 was used. All X^- yields exhibit a nearly linear dependence on the calibration gas anion signal.

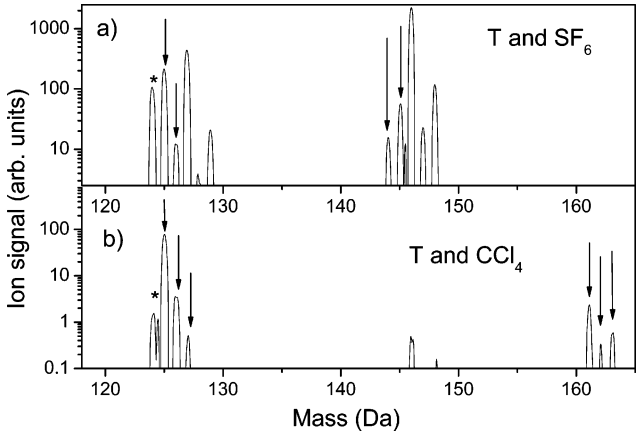

Figure 9. Mass spectra in the range from 118 to 165 Da recorded at an electron energy close to 0 eV energy for thymine using two different calibration gases (9a: SF_6; 9b: CCl_4). Peaks which are only observed in the presence of thymine and one of the calibration gases are indicated by the arrows. The fragment ion at mass 124 Da designated by the star has a resonance close to 0 eV which increases only in the presence of SF_6. Other peaks observed in Figure 9a are anions formed via (dissociative) EA to SF_6. The small contribution at 146 Da in Figure 9b is due to the small impurity with SF_6 in the gas inlet when using CCl_4.

reactions within our detection limit:

$$C + SF_6^- \rightarrow (C-H)^- + HF + SF_5 \quad (6a)$$

$$T + (Cl^-/CCl_4) \rightarrow (T-H)^- + HCl \quad (6b)$$

$$T + SF_6^- \rightarrow (T-H)^- + HF + SF_5 \quad (6c)$$

$$\rightarrow (T-2H)^- + 2HF + SF_4 \quad (6d)$$

All reactions lead to a signal contribution at 0 eV since the corresponding primary anions, that is, Cl^- and SF_6^-, have strong s-wave attachment cross sections at very low electron energies. The dependence of the intensity of the 0 eV peaks as a function of the Cl^- or SF_6^- ion yield is shown in Figure 8. For these measurements, we increased the partial pressure of the calibrant gas (CCl_4 or SF_6) from 0 up to 2×10^{-5} Pa. In all cases, we observe a more or less linear dependence between the calibrant gas ion yield and the product anions formed via reactions 6a−6d. It is remarkable that we were not able to detect any anion molecule reactions between cytosine and Cl^- whereas Cl^- reacts strongly with thymine and Uracil. The observation of additional 0 eV peaks in the presence of other gas molecules was already reported in the article of Drexel et al.,[57] where electrons that are released via autodetachment from $C_2Cl_4^-$ in sufficiently strong electric fields generate O^- from O_2 at apparently 0 eV. This effect, called Trojan horse ionization, can clearly be ruled out in the present study since both Cl^- and SF_6^- have much smaller autodetachment rates compared to $C_2Cl_4^-$. Mass spectra recorded in the mass range from 1 Da up to 165 Da at the electron energy close to 0 eV exhibit other products formed by anion molecule reactions between thymine and the calibration gas. For SF_6 used as a calibration gas, additional ions are formed in the interaction with thymine at mass 144 and 145 Da (Figure 9a). When CCl_4 is used as the calibration gas, we observe peaks at 161, 162, and 163 Da which appear in the mass spectra (shown in Figure 9b).

Conclusion

We performed free-electron attachment to gas-phase cytosine and thymine in the electron energy range from about 0 to 14 eV. As for other biomolecules, like Uracil,[5,6] glycine,[58] formic acid, and acetic acid,[59] no parent anions were observed and the most abundant fragment anion is the closed-shell dehydrogenated molecule. Several fragment anions that are formed with decomposition of the ring structure of the molecules were observed exclusively for one of the two molecules. In addition, the ion efficiency curves of fragment anions that were formed via DEA to both molecules differ substantially which can be explained by the different molecular structure of C and T. However, surprisingly large differences are also observed in the comparison to DEA to thymine and Uracil, since both molecules have the same ring structure.

$(C-H)^-$ is formed with a similar cross section like $(U-H)^-$ from Uracil[5,6] and $(G-H)^-$ from glycine[58] whereas the cross section for $(T-H)^-$ is about 3 times higher. The present ion yield of $(T-H)^-$ agrees well with results of Abouaf et al.[29] on DEA to thymine using a hemispherical electron monochromator. The present results for DEA to cytosine and thymine deviate in several cases from the observations made by Huels et al.[27] The observation of stable parent ions of C and T in ref 27 is likely to be the result of a problem with mass determination or the presence of SF_6 in the interaction region of the thymine and the electrons. The different anion yields of less abundant fragments can be explained by different experimental conditions such as the extraction fields of the anions from the collision chamber and the different temperatures used to vaporize the DNA bases (in ref 27, 120−180 °C and for the present measurements, 180−200 °C).

It is a remarkable fact that DEA to free T and C below 3 eV effectively leads to bond breaking at positions where T and C form links to the neighboring molecules in DNA leading to $(C-H)^-$ and $(T-H)^-$. However, it has to be considered that the most intense contribution at 1 eV in the gas-phase $(T-H)^-$ ion yield may arise from initially dipole bound anions[29,30] which are suppressed in DNA environment because of the preference of valence ion formation. Of great relevance for DNA damage may be the large variety of (valence bound) fragment anions observed in the present experiments which are formed mainly at higher electron energies larger than 8 eV. These results represent the bridge to the condensed films of isolated nucleobases,[31] where desorption of anions below 42 Da has been observed at similar electron energies. These films of nucleobases represent a more lifelike environment than the isolated hot

molecules in the gas phase. Anion formation of heavier fragments may also take place at lower electron energies in condensed films but because of insufficient kinetic energy the formed anions cannot desorb from the surface. The experiments of Sanche and co-workers[3] clearly showed that strand breaks of DNA are formed resonantly at electron energies of about 10 eV. This was explained by initial DEA to DNA components. The present gas-phase experiments confirm strong decomposition of thymine and cytosine into fragment anions and neutral radicals at low electron energies. Several fragment anions reveal resonances at about 10 eV (for example, O^-) where Sanche and co-workers observed a maximum of the strand break yields.[3]

Acknowledgment. This work has been supported by the FWF, and ÖNB, Wien, Austria and European Commission, Brussels. Partial support is also acknowledged by the Grant of the Grant Agency of the Czech Republic (GA203/02/0737).

References and Notes

(1) International Commission on Radiation Units and Measurements. ICRU Report 31; ICRU: Washington, DC, 1979.

(2) Cobut, V.; Fongillo, Y.; Patau, J. P.; Goulet, T.; Fraser, M.-J.; Jay-Gerin, J.-P. *Radiat. Phys. Chem.* **1998**, *51*, 229.

(3) Boudaiffa, B.; Cloutier, P.; Hunting, D.; Huels, M. A.; Sanche, L. *Science* **2000**, *287*, 1658.

(4) De Vries, J.; Hoekstra, R.; Morgenstern, R.; Schlathölter, T. *J. Phys. B: At. Mol. Opt. Phys.* **2002**, *35*, 4373.

(5) Hanel, G.; Gstir, B.; Denifl, S.; Scheier, P.; Probst, M.; Farizon, B.; Farizon, M.; Illenberger E.; Märk T. D. *Phys. Rev. Lett.* **2003**, *90*, 1888104−1.

(6) Denifl, S.; Ptasińska, S.; Hanel, G.; Gstir, B.; Probst, M.; Scheier, P.; Märk T. D. *J. Chem. Phys.* **2004**, *120*, 6557.

(7) Aflatooni, K.; Gallup, G. A.; Burrow, P. D. *J. Phys. Chem.* **1998**, *102*, 6205.

(8) Desfrancois, C.; Periquet, V.; Bouteilleir, Y.; Schermann, J. P. *J. Chem. Phys.* **1996**, *104*, 7792.

(9) Desfrancois, C.; Abdoul-Carime, H.; Schermann, J. P. *J. Phys. Chem.* **1998**, *102*, 1274.

(10) Periquet, V.; Moreau, A.; Carles, S.; Schermann, J. P.; Desfrancois, C. *J. Electron Spectrosc. Relat. Phenom.* **2000**, *106*, 141.

(11) Desfrancois, C.; Abdoul-Carime, H.; Khelifa, N.; Schermann, J. P. *Phys. Rev. Lett.* **1994**, *73*, 2436.

(12) Hendricks, J. H.; Lyapustina, S. A.; de Clercq, H. L.; Snodgrass, J. T.; Bowen, K. H. *J. Chem. Phys.* **1996**, *104*, 7788.

(13) Hendricks, J. H.; Lyapustina, S. A.; de Clercq, H. L.; Bowen, K. H. *J. Chem. Phys.* **1998**, *108*, 8.

(14) Schiedt, J.; Weinkauf, R.; Neumark, D. M.; Schlag, E. W. *Chem. Phys.* **1998**, *239*, 511.

(15) Oyler, N. A.; Adamowicz, L. *J. Phys. Chem.* **1993**, *97*, 11122.

(16) Smith, D. M. A.; Jalbout, A. F.; Smets, J.; Adamowicz, L. *Chem. Phys.* **2000**, *260*, 45.

(17) Colson, A. O.; Sevilla, M. D. *Int. J. Radiat. Biol.* **1995**, *67*, 627.

(18) Wetmore, S. D.; Boyd, R. J.; Eriksson, L. A. *Chem. Phys. Lett.* **2000**, *322*, 129.

(19) Wesolowski, S. S.; Leininger, M. L.; Pentchev, P. N.; Schaefer, H. F., III. *J. Am. Chem. Soc.* **2001**, *123*, 4023.

(20) Russo, N.; Toscano, M.; Grand, A. *J. Comput. Chem.* **2000**, *21*, 1243.

(21) Li, X.; Cai, Z.; Sevilla, M. D. *J. Phys Chem. A* **2002**, *106*, 1596.

(22) Becke, A. D. *J. Chem. Phys.* **1993**, *98*, 1372.

(23) Li, X.; Cai, Z.; Sevilla, M. D. *J. Phys Chem. A* **2002**, *106*, 9345.

(24) Chen, E. C. M.; Chen, E. S. D.; Wentworth, W. E. *Biochem. Biophys. Res. Commun.* **1990**, *171*, 97.

(25) Wiley: J. R.; Robinson, J. M.; Ehdaie, S.; Chen, E. C. M.; Chen, E. S. D.; Wentworth, W. E. *Biochem. Biophys. Res. Commun.* **1991**, *180*, 841.

(26) Chen, E. C. M.; Chen, E. S. D. *J. Phys. Chem. B* **2000**, *104*, 7835.

(27) Huels, M. A.; Hahndorf, I.; Illenberger, E.; Sanche, L. *J. Chem. Phys.* **1998** *108*, 1309.

(28) Gohlke, S.; Illenberger, E. *Europhys. News* **2002**, *33*, 207.

(29) Abouaf, R.; Pommier, J.; Dunet, H. *Int. J. Mass Spectrosc.* **2003**, *226*, 397.

(30) Scheer, A. M.; Aflatooni, K.; Gallup, G. A.; Burrow, P. D. *Phys. Rev. Lett.* **2004**, *92*, 068102.

(31) Abdoul-Carime, H.; Cloutier, P.; Sanche, L. *Radiat. Res.* **2001**, *155*, 625.

(32) Denifl, S.; Ptasińska, S.; Cingel, M.; Matejcik, S.; Scheier, P.; Märk, T. D. *Chem. Phys. Lett.* **2003**, *377*, 74.

(33) Muigg, D.; Denifl, G.; Stamatovic, A.; Märk, T. D. *Chem. Phys.* **1998**, *239*, 409.

(34) Matejcik, S.; Senn, G.; Scheier, P.; Kiendler, A.; Stamatovic, A.; Märk, T. D. *J. Chem. Phys.* **1997**, *107*, 8955.

(35) Christophorou, L. G.; Olthoff, J. K. *Int. J. Mass Spectrosc.* **2001**, *205*, 27.

(36) *Gallup, G. A.; Aflatooni, K.; Burrow, P. D. J. Chem. Phys.* **2003**, *118*, 2562.

(37) Klar, D.; Ruf, M.-W.; Hotop, H. *Int. J. Mass Spectrosc.* **2001**, *205*, 93.

(38) Hotop, H. Ruf, M.-W.; Allan, M.; Fabrikant, I. I. *Adv. At. Mol. Opt. Phys.* **2003**, *49*, 85.

(39) Feil, S.; Gluch, K.; Matt-Leubner, S.; Scheier, P.; Limtrakul, J.; Probst, M.; Deutsch, H.; Becker, K.; Stamatovic, A.; Märk, T. D. *J. Phys. B*, submitted.

(40) Cicman, P.; Francis, M.; Skalny. J. D.; Märk, T. D. *Int. J. Mass Spectrosc.* **2003**, *223/224*, 271.

(41) Rodgers, M. T.; Campbell, S.; Marzluff, E. M.; Beauchamp, J. L. *Int. J. Mass Spectrosc. Ion Proc.* **1994**, *137*, 121.

(42) Hahndorf, I.; Illenberger, E. *Int. J. Mass Spectrosc.* **1997**, *167/168*, 87.

(43) Chen, E. S. D.; Chen, E. C. M.; Sane, N. *Biochem. Biophys. Res. Commun.* **1998**, *246*, 228.

(44) Abdoul-Carime, H.; Gohlke, S.; Illenberger, E. *Phys. Rev. Lett.* **2004**, *92*, 168103.

(45) Abouaf, R. private communications.

(46) Illenberger, E. *Gaseous Molecular Ions*, Vol. 2; Steinkopff Verlag: Darmstadt, Germany, 1992.

(47) Head-Gordon, M.; Pople, J. A.; Frisch, M. J. *Chem. Phys. Lett.* **1988**, *153*, 503.

(48) McLean, A. D.; Chandler, G. S. *J. Chem. Phys*. **1980**, *72*, 5639.

(49) Krishnan, R.; Binkley, J. S.; Seeger, R.; Pople, J. A. *J. Chem. Phys.* **1980**, *72*, 650.

(50) Curtiss, L. A.; Raghavachari, K.; Pople, J. A. *J. Chem. Phys.* **1993**, *98*, 1293.

(51) Ptasińska, S.; Denifl, S.; Scheier, P.; Märk, T. D. to be submitted.

(52) Frisch, M. J.; Trucks, G. W.; Schlegel, H. B.; Scuseria, G. E.; Robb, M. A.; Cheeseman, J. R.; Zakrzewski, V. G.; Montgomery, J. A., Jr.; Stratmann, R. E.; Burant, J. C.; Dapprich, S.; Millam, J. M.; Daniels, A. D.; Kudin, K. N.; Strain, M. C.; Farkas, O.; Tomasi, J.; Barone, V.; Cossi, M.; Cammi, R.; Mennucci, B.; Pomelli, C.; Adamo, C.; Clifford, S.; Ochterski, J.; Petersson, G. A.; Ayala, P. Y.; Cui, Q.; Morokuma, K.; Malick, D. K.; Rabuck, A. D.; Raghavachari, K.; Foresman, J. B.; Cioslowski, J.; Ortiz, J. V.; Stefanov, B. B.; Liu, G.; Liashenko, A.; Piskorz, P.; Komaromi, I.; Gomperts, R.; Martin, R. L.; Fox, D. J.; Keith, T.; Al-Laham, M. A.; Peng, C. Y.; Nanayakkara, A.; Gonzalez, C.; Challacombe, M.; Gill, P. M. W.; Johnson, B. G.; Chen, W.; Wong, M. W.; Andres, J. L.; Head-Gordon, M.; Replogle, E. S.; Pople, J. A. *Gaussian 98*, revision A.11: Gaussian, Inc.: Pittsburgh, PA, 1998.

(53) Jensen, F. *Introduction to Computational Chemistry*; John Wiley & Sons: Chichester, U.K., 1999.

(54) Levine, I. N. *Quantum Chemistry*; Prentice Hall: Upper Saddle River, NJ, 1991.

(55) Ptasińska, S.; Denifl, S.; Scheier, P.; Märk, T. D. *Phys. Rev. Lett.* submitted.

(56) Gohlke, S.; Abdoul-Carime, H.; Illenberger, E. *Chem. Phys. Lett.* **2003**, *380*, 595.

(57) Drexel, H.; Sailer, W.; Grill, V.; Scheier, P.; Illenberger, E.; Märk, T. D. *J. Chem. Phys.* **2003**, *118*, 7394.

(58) Ptasińska, S.; Denifl, S.; Abedi, A.; Scheier, P.; Märk, T. D. *Anal. Bioanalytical Chem.* **2003**, *377*, 1115.

(59) Pelc, A.; Sailer, W.; Scheier, P.; Mason, N. J.; Illenberger, E.; Märk, T. D. *Vacuum* **2003**, *70*, 429.